Use the form (53) and assume $t \geqq \alpha_1+\alpha_2$. It is always easy to integrate over one component of $\mathbf{k}$, say k_2, by use of the formula,

$$\frac{1}{\pi}\int_0^\pi dk_2 \frac{\cos nk_2}{x-\cos k_2} = \frac{(x-(x^2-1)^{1/2})^n}{(x^2-1)^{1/2}}. \quad \text{(D1)}$$

Those of the resulting integrals which are not trivial may be transformed by the substitutions,

$$k_1 = \pi - 2\theta,$$
$$0 \leqq n_2^2 \equiv \frac{2\alpha_1}{t+\alpha_1+\alpha_2} \leqq \frac{2\alpha_1}{t+\alpha_1-\alpha_2} \equiv n_1^2 \leqq 1, \quad \text{(D2)}$$

into expressions of the type,

$$\frac{2}{\pi}\int_0^{\pi/2} d\theta \frac{(\sin\theta)^{2\nu}}{[(1-n_1^2\sin^2\theta)(1-n_2^2\sin^2\theta)]^{1/2}}, \quad \nu \text{ integral}, \quad \text{(D3)}$$

times certain factors involving the α_l. These integrals in turn yield to the elliptic substitution,[27]

$$\mathrm{sn}^2 u = \frac{(1-n_2^2)\sin^2\theta}{1-n_2^2\sin^2\theta}, \quad \text{(D4)}$$

giving the results (64).

[27] P. F. Byrd and M. D. Friedman, Ref. 12, Eqs. 284, 336, and 337.

PHYSICAL REVIEW VOLUME 132, NUMBER 1 1 OCTOBER 1963

Magnetic-Field Dependence of Free-Carrier Absorption in Semiconductors*

J. K. FURDYNA
National Magnet Laboratory,† Massachusetts Institute of Technology, Cambridge, Massachusetts

AND

M. E. BRODWIN
Department of Electrical Engineering, Northwestern University, Evanston, Illinois

(Received 13 May 1963)

A plane-wave semiclassical analysis of the amplitude of an electromagnetic wave transmitted through a semiconductor in the presence of a magnetic field is discussed and some theoretical predictions are compared with experimental measurements. The Faraday and the Voigt configurations, longitudinal and transverse, respectively, are specifically considered. The theoretical results, obtained formally in terms of the high-frequency conductivity tensor, are applied to the isotropic, one-carrier semiconductor model. The general expression, covering all ranges of frequency and magnetic field within the extent of validity of the model, is derived and reduced to simple forms applicable to specific experimental situations. The problem is then generalized to ellipsoidal surfaces of constant energy, and to systems involving more than one type of carrier. Results of room temperature microwave experiments carried out in the Faraday configuration on silicon and germanium show, in general, good agreement with the theoretical analysis. Effects of magnetodichroism, observed in *n*-type silicon in this configuration, are reported. It is finally noted that the theoretical analysis of the Voigt configuration predicts the major features of the line shapes observed in far infrared experiments by other workers.

INTRODUCTION

MAGNETO-OPTICAL phenomena involving changes in the state of polarization of a wave, such as the Faraday or the Voigt effects, have recently received much attention as experimental tools for investigating transport properties of semiconductors. In this article, we analyze the magnetic-field dependence of the total absorption associated with the above phenomena, in the attempt to see what further information can be obtained by measuring transmitted amplitude as a function of the field. It will be shown that the effect provides a means of investigating the magnetic-field dependence of the diagonal component of the conductivity tensor, and represents in fact a modified high-frequency version of magnetoresistance. The changes in the amplitude of the transmitted wave can be quite pronounced in the free-carrier region and, in general, involve simple measuring techniques. It is thus worthwhile to consider the effect as a useful high-frequency method for the study of galvanomagnetic properties.

We will first outline a plane-wave semiclassical analysis of the case when an initially linearly polarized wave travels along the direction of an applied magnetic field. This situation gives rise to the Faraday effect, and will be referred to as the Faraday configuration. We will then consider the case of propagation transverse to the applied field, i.e., the Voigt configuration. Results of some microwave and infrared experiments carried out

* Initial work supported by the Advanced Research Projects Agency through the Northwestern University Materials Research Center.
† Supported by the U. S. Air Force Office of Scientific Research.

in these configurations will finally be compared with the theoretical analysis.

THEORY

A. The Faraday Configuration

1. *General Formulation*

The attenuation constant β of a nonmagnetic medium can be expressed in terms of the effective complex dielectric constant $\epsilon_{\text{eff}}=\epsilon'+i\epsilon''$ as

$$\beta=\omega(\tfrac{1}{2}\mu_0)^{1/2}[(\epsilon'^2+\epsilon''^2)^{1/2}-\epsilon']^{1/2}, \tag{1}$$

where μ_0 is the permeability of free space, ω the frequency, and ϵ' and ϵ'' are real. The mks system is used throughout this paper. In analyzing the Faraday configuration, one considers the incident linearly polarized wave in terms of its contrarotating circularly polarized components, each of which is characterized by a different ϵ_{eff} and β. It is convenient to formulate the problem in terms of the high-frequency conductivity tensor. For isotropic materials in a magnetic field,

$$\sigma=\begin{bmatrix}\sigma_{11} & \sigma_{12} & 0\\ -\sigma_{12} & \sigma_{11} & 0\\ 0 & 0 & \sigma_{33}\end{bmatrix}, \tag{2}$$

where the coordinate system is defined by taking the direction of magnetic field as axis 3. The diagonal component can be written $\sigma_{11}=\sigma_{11}(0)-\Delta\sigma$, where $\Delta\sigma$ contains the magnetic-field dependence, and $\sigma_{11}(0)$ is the high-frequency conductivity at zero field.

The real and imaginary parts of the effective dielectric constant for the two senses of polarization can now be written[1]

$$\epsilon_{\pm}'=\epsilon_{st}'+[(\sigma_{11}''\pm\sigma_{12}')/\omega], \tag{3}$$

$$\epsilon_{\pm}''=(\sigma_{11}'\mp\sigma_{12}'')/\omega. \tag{4}$$

Here ϵ_{st}' is the dielectric constant of the material without the free-carrier contribution, and the single and double prime denote real and imaginary parts. The upper and lower signs refer, respectively, to the right- and left-handed circular polarization.

The major axis of the elliptically polarized wave transmitted at field B is given as the sum of the amplitudes of the two components $E(B)=E_0(e^{-\beta_+ z}+e^{-\beta_- z})$ where $2E_0$ is the incident amplitude and z the thickness of the specimen. In the absence of the magnetic field, the transmitted amplitude is given by $E(0)=2E_0e^{-\beta_0 z}$, β_0 being the zero-field attenuation constant. It then follows that

$$\frac{E(B)}{E(0)}=\frac{\exp(-\beta_+ z)+\exp(-\beta_- z)}{2\exp(-\beta_0 z)}=\exp[\tfrac{1}{2}(2\beta_0-\beta_+-\beta_-)z]. \tag{5}$$

Equation (5) is obtained by neglecting second-order terms in $\frac{1}{2}(\beta_+-\beta_-)z$, which, in general, is a very good approximation.

2. *Small Losses*

The case of small loss tangent, $\epsilon''/\epsilon'\ll 1$, will be discussed for three regions: $\tau^{-1}\gg\omega$, ω_c; $\omega_c\gg\tau^{-1}$, ω; and $\omega\gg\omega_c$, τ^{-1}, where τ^{-1} and ω_c are the scattering and the cyclotron frequencies, respectively. A convenient general expression can be obtained for the three regions,

$$\ln\frac{E(B)}{E(0)}=\tfrac{1}{2}z\left(\frac{\mu_0}{\epsilon_{st}'}\right)^{1/2}\Delta\sigma'=\beta_0 z\frac{\Delta\sigma'}{\sigma_{11}'(0)}. \tag{6}$$

Equation (6) was derived under the condition $\omega_p^2/(\omega\Omega)\ll 1$, where Ω designates τ^{-1}, ω, or ω_c, whichever of these is the largest in the given region. Here ω_p is the classical plasma frequency $[ne^2/(m^*\epsilon_{st}')]^{1/2}$, where n is the carrier density and m^* the effective mass. The above condition guarantees that the loss tangent is small and that $\epsilon_{\pm}'$ is positive.[2]

In order to study the behavior of Eq. (6), it is instructive to express $\Delta\sigma'$ in terms of the one-electron model, assuming isotropic effective mass m^* and isotropic relaxation time in the form $\tau=\tau_0\epsilon^p$, where ϵ is the carrier energy relative to the band edge.[3] Then

$$\Delta\sigma'=\frac{ne^2}{m^*}\left\langle\frac{\tau(1+\omega_c^2\tau^2-3\omega^2\tau^2)\omega_c^2\tau^2}{(1+\omega^2\tau^2)[(1+\omega_c^2\tau^2+\omega^2\tau^2)^2-4\omega^2\omega_c^2\tau^4]}\right\rangle. \tag{7}$$

For a Maxwell-Boltzmann distribution,

$$\langle g(x)\rangle\equiv\frac{4}{3\sqrt{\pi}}\int_0^\infty g(x)x^{3/2}e^{-x}dx,$$

where $x=\epsilon/kT$.

Equation (7) can be readily reduced to any range of signal, collision, and cyclotron frequencies. Thus, when the collision frequency is high ($\tau^{-1}\gg\omega$, $\tau^{-1}\gg\omega_c$, typical of microwave experiments at room temperature),

$$\ln\frac{E(B)}{E(0)}=\tfrac{1}{2}z\left(\frac{\mu_0}{\epsilon_{st}'}\right)^{1/2}\frac{ne^2}{m^*}\omega_c^2\langle\tau^3\rangle,$$

$$=\tfrac{1}{2}z\left(\frac{\mu_0}{\epsilon_{st}'}\right)^{1/2}\sigma_0\mu_H\mu_d B^2\frac{\langle\tau^3\rangle}{\langle\tau^2\rangle\langle\tau\rangle},$$

$$=\beta_0 z\mu_H\mu_d B^2\frac{\langle\tau^3\rangle}{\langle\tau^2\rangle\langle\tau\rangle}, \tag{8}$$

[1] B. Lax and L. M. Roth, Phys. Rev. **98**, 549 (1955). See also B. Lax and J. G. Mavroides, in *Solid State Physics*, edited by F. Seitz and D. Turnbull (Academic Press Inc., New York, 1960), Vol. 11, p. 261.

[2] In the present article we do not discuss explicitly the narrow range where $0>\epsilon_{\pm}''/\epsilon_{\pm}'>(-1)$. In this region of extreme attenuation experiments involving transmission are impractical. Moreover, if the inequality holds for one sense of polarization, but not the other (helicon waves), Eq. (5) does not apply.

[3] Components of the conductivity tensor in terms of this model are given explicitly in, e.g., J. K. Furdyna and M. E. Brodwin, Phys. Rev. **124**, 740 (1961).

where μ_H and μ_d are the Hall and drift mobilities $e\langle\tau^2\rangle/(m^*\langle\tau\rangle)$ and $e\langle\tau\rangle/m^*$, respectively, and σ_0 is the dc conductivity $ne^2\langle\tau\rangle/m^*$.

In the high-magnetic-field region ($\omega_c\gg\omega$, $\omega_c\gg\tau^{-1}$), the expression is given by

$$\ln\frac{E(B)}{E(0)}=\tfrac{1}{2}z\left(\frac{\mu_0}{\epsilon_{st}'}\right)^{1/2}\frac{ne^2}{m^*}\frac{1}{\omega_c^2}\left\langle\frac{1}{\tau}\left(\frac{\omega_c^2\tau^2}{1+\omega^2\tau^2}-1\right)\right\rangle, \quad (9)$$

which approaches $\frac{1}{2}z(\mu_0/\epsilon_{st}')^{1/2}\sigma_{11}'(0)=\beta_0 z$, illustrating the disappearance of free-carrier absorption in the high-field limit.

In the range $\omega\gg\tau^{-1}$, $\omega\gg\omega_c$, characteristic of infrared or low-temperature microwave experiments, the amplitude ratio is given by

$$\ln\frac{E(B)}{E(0)}=-\tfrac{3}{2}z\left(\frac{\mu_0}{\epsilon_{st}'}\right)^{1/2}\frac{ne^2}{m^*}\frac{\omega_c^2}{\omega^4}\left\langle\frac{1}{\tau}\right\rangle=-3\beta_0 z\frac{\omega_c^2}{\omega^2}. \quad (10)$$

At cyclotron resonance ($\omega=\omega_c\gg\tau^{-1}$), Eq. (7) reduces to the well-known dependence

$$\ln\frac{E(B)}{E(0)}=-\tfrac{1}{4}z\left(\frac{\mu_0}{\epsilon_{st}'}\right)^{1/2}\frac{ne^2}{m^*}\langle\tau\rangle$$

$$=-\tfrac{1}{4}z\left(\frac{\mu_0}{\epsilon_{st}'}\right)^{1/2}\sigma_0=-\tfrac{1}{2}\beta_0 z\omega^2\langle\tau\rangle\left\langle\frac{1}{\tau}\right\rangle^{-1}. \quad (11)$$

Note that Eqs. (10) and (11) indicate a decrease of amplitude with increasing magnetic field, in contrast with Eqs. (8) and (9). Note further, that the amplitude ratio depends essentially on $\langle\tau^3\rangle$ in the case of short collision times, on $\langle\tau^{-1}\rangle$ in the limit of high frequency or field, and on $\langle\tau\rangle$ in the particular instance of cyclotron resonance. In intermediate ranges of τ^{-1}, ω and ω_c, the amplitude behavior is more complicated, but can be obtained by an appropriate expansion of Eq. (7).

3. *High Losses*

The range of very high values of the loss tangent ϵ''/ϵ' will be considered for the case when the collision frequency exceeds both the cyclotron frequency and the frequency of the wave, $\tau^{-1}\gg\omega_c$, $\tau^{-1}\gg\omega$. In this range, the high-loss approximation of the amplitude ratio can be written in terms of the $\boldsymbol{\sigma}$ tensor as

$$\ln\frac{E(B)}{E(0)}=\tfrac{1}{2}z\left[\frac{\omega\mu_0}{2\sigma_{11}'(0)}\right]^{1/2}\Delta\sigma'=\tfrac{1}{2}\beta_0 z\frac{\Delta\sigma'}{\sigma_{11}'(0)}. \quad (12)$$

For the frequency range considered here, the one-carrier model then yields

$$\ln\frac{E(B)}{E(0)}=\tfrac{1}{2}z(\tfrac{1}{2}\omega\mu_0\sigma_0)^{1/2}\omega_c^2\frac{\langle\tau^3\rangle}{\langle\tau\rangle}=\tfrac{1}{2}\beta_0 z\omega_c^2\frac{\langle\tau^3\rangle}{\langle\tau\rangle}. \quad (13)$$

Thus far, the derivation has neglected the problem of reflections at interfaces. This is justified for the low-loss region where reflections are determined primarily by ϵ_{st}'. However, in the present case, reflections are mostly due to the sample conductivity, and hence will manifest a significant dependence on the magnetic field. The effect of taking reflections into account amounts to replacing z with $z+\delta$ in Eqs. (12) and (13), where δ is the skin depth.[4]

The region of high frequencies or high fields is not discussed in this section. The value of the loss tangent is itself a function of the parameters $\omega\tau$ and $\omega_c\tau$ [as can be seen from Eqs. (3) and (4)], and in general decreases as these quantities are increased. Hence, in the limit $\omega\tau\gg1$ or $\omega_c\tau\gg1$ the situation will generally belong to the range of small losses, described by the equations in the previous section.

4. *Connection with the Faraday Rotation*

It is possible to correlate the amplitude ratio with the simultaneously occurring Faraday rotation θ.[3,5] For low-loss materials, as well as lossy samples with $z\gg\delta$,

$$\frac{1}{\theta}\ln\frac{E(B)}{E(0)}=\frac{\Delta\sigma'}{\sigma_{12}'}. \quad (14)$$

In terms of the simple model, this reduces to

$$\frac{\Delta\sigma'}{\sigma_{12}'}=\omega_c\langle\tau\rangle\frac{\langle\tau^3\rangle}{\langle\tau^2\rangle\langle\tau\rangle}=\mu_d B\frac{\langle\tau^3\rangle}{\langle\tau^2\rangle\langle\tau\rangle}$$

$$\text{for } \tau^{-1}\gg\omega_c,\ \tau^{-1}\gg\omega; \quad (14a)$$

$$\frac{\Delta\sigma'}{\sigma_{12}'}=\omega_c\left\langle\frac{\tau}{1+\omega^2\tau^2}\right\rangle=\mu_d B\frac{\sigma_{11}'(0)}{\sigma_0}$$

$$\text{for } \omega_c\gg\tau^{-1},\ \omega_c\gg\omega; \quad (14b)$$

and

$$\frac{\Delta\sigma'}{\sigma_{12}'}=-3\frac{\omega_c}{\omega^2}\left\langle\frac{1}{\tau}\right\rangle \quad \text{for } \omega\gg\tau^{-1},\ \omega\gg\omega_c. \quad (14c)$$

This correlation can be used to eliminate several parameters from the measurement, viz. the carrier concentration, the lattice dielectric constant, and the thickness. The elimination of the thickness z is of interest, since this, in turn, greatly reduces the error due to multiple internal reflections, standing waves, and certain geometric irregularities. It is, further, possible to apply Eq. (14) to measurements on powders, where the active optical path length is unknown.

Similar correlations are possible with other quantities, such as Faraday ellipticity, total absorption, or phase shift.

---

[4] To include the effect of reflections, we have followed the magneto-Kerr-effect formulation of R. J. Vernon, M. S. thesis, Northwestern University, 1961 (unpublished).

[5] J. K. Furdyna and S. Broersma, Phys. Rev. **120**, 1995 (1960).

5. *Anisotropy of the Effective Mass*

For an arbitrary orientation of magnetic field in crystals characterized by anisotropic constant energy surfaces, σ_{11} generally differs from σ_{22} by terms quadratic in B. Hence our analysis, which involves these terms and which assumes $\sigma_{11}=\sigma_{22}$, does not hold rigorously. In this case a more elaborate treatment, resolving the incident field pattern into appropriate elliptically polarized components, is necessary even for the low-field limit. The procedure recently developed by Donovan and Webster[6] for the Faraday effect may be extended to the present problem.

However, when B is applied along certain crystallographic directions of high symmetry (e.g. the [111] or [100] axes in n-type silicon and germanium), σ_{11} becomes equal to σ_{22}, and Eqs. (6) and (12) are valid. Now, however, the forms of σ_{11} are different for each orientation of B.[7] Effective-mass anisotropy can thus be obtained from the amplitude variation.

Using n-type silicon as an example it can be shown, upon substituting the high-frequency conductivity tensor in Eq. (6), that for magnetic field in the [100] direction, ω_c^2/m^* in Eq. (8) must be replaced by the form

$$\frac{\omega_c^2}{m^*}\rightarrow\frac{e^2B^2(m_1^2+m_1m_2+m_2^2)}{3m_1^2m_2^3}, \tag{15a}$$

whereas for the field along the [111] direction, ω_c^2/m^* must be written

$$\frac{\omega_c^2}{m^*}\rightarrow\frac{e^2B^2(m_1+2m_2)(2m_1+m_2)}{9m_1^2m_2^3}, \tag{15b}$$

where m_1 and m_2 are the longitudinal and transverse components of the effective mass tensor, respectively. Note that Eq. (15b) substituted in Eq. (8) will yield an expression in terms of σ_0, μ_H and μ_d identical in form to the isotropic case, where now $\mu_H=(m_1+2m_2)e\langle\tau^2\rangle/[(2m_1+m_2)m_2\langle\tau\rangle]$ and $\mu_d=(2m_1+m_2)e\langle\tau\rangle/(3m_1m_2)$.

Equations for other ranges of ω and ω_c can be similarly derived by introducing the components of the conductivity tensor appropriate to the given orientation in Eq. (6).

6. *Degenerate Bands and Minority Carriers*

In the presence of more than one type of carrier, Eq. (7) must be generalized to the form

$$\Delta\sigma'=\sum_i\frac{n_ie_i^2}{m_i^*}\times\left\langle\frac{\tau_i(1+\omega_{ci}^2\tau_i^2-3\omega^2\tau_i^2)\omega_{ci}^2\tau_i^2}{(1+\omega^2\tau_i^2)[(1+\omega_{ci}^2\tau_i^2+\omega^2\tau_i^2)^2-4\omega^2\omega_{ci}^2\tau_i^4]}\right\rangle, \tag{16}$$

where i refers to the carrier type.

[6] B. Donovan and J. Webster, Proc. Phys. Soc. (London) **79**, 46 and 1081 (1962).

[7] To obtain the high-frequency conductivity tensor for a given orientation of magnetic field, see, e.g., B. Lax, H. J. Zeiger, and R. N. Dexter, Physica **20**, 818 (1954).

Since the amplitude ratio depends on the diagonal component of the conductivity tensor, the effects of electrons and holes are additive, in contrast to the Faraday rotation or ellipticity. This must be taken into account in working with intrinsic and near-intrinsic materials, particularly if the minority carrier mobility is large.

In the case of band degeneracy, the effect of light holes on the amplitude ratio is exceedingly important at low field. This can be easily demonstrated for the low-field and low-frequency limit, in which Eq. (16) becomes

$$\Delta\sigma'=\frac{n_2e^2}{m_2}\omega_{c2}^2\langle\tau^3\rangle\left(1+\frac{n_1}{n_2}\frac{m_2^3}{m_1^3}\right)\approx\frac{n_2e^2}{m_2}\omega_{c2}^2\langle\tau^3\rangle\left[1+\left(\frac{m_2}{m_1}\right)^{3/2}\right], \tag{17}$$

where subscripts 1 and 2 refer to the heavy and light holes, respectively. Here scattering times and scattering mechanisms for the two types are assumed the same, and in the last form of the expression n_1/n_2 is assumed to be given by the density-of-states ratio $(m_1/m_2)^{3/2}$. It is thus clear that, if the two masses are considerably different (as, e.g., in p-type germanium), the effect is determined almost entirely by the light hole.

Another interesting property of Eq. (16) is the saturation of the light-hole contribution in the region where $\omega_{c2}\tau$ is no longer small, but $\omega_{c1}\tau\ll1$ still holds. Then

$$\Delta\sigma'=\frac{n_2e^2}{m_2}\omega_{c2}^2\left[\left\langle\frac{\tau^3}{1+\omega_{c2}^2\tau^2}\right\rangle+\left(\frac{m_2}{m_1}\right)^{3/2}\langle\tau^3\rangle\right]. \tag{18}$$

It is easily seen that the initial dropping off of the amplitude ratio from quadratic B dependence is even less sensitive to the heavy hole.

Expressions for other ranges can be similarly obtained by reducing Eq. (16). The behavior is in general closely analogous to magnetoresistance in degenerate bands. It must be emphasized, however, that in the present case the quantity measured lends itself to theoretical analysis much more readily. For instance, in the low-field and low-frequency limit, the amplitude ratio depends on the single $\langle\tau^3\rangle$ magnetoconductivity term, contrasted with the inseparable combination $(\langle\tau^3\rangle-a\langle\tau^2\rangle^2/\langle\tau\rangle)$ encountered in dc magnetoresistance, where the quantity a represents the fact that the relative contribution from the two bands is different to each of the averages.

B. The Voigt Configuration

Experiments involving propagation transverse to the magnetic field are of great interest in the presence of anisotropy, since in this configuration one can vary

the relative orientation of magnetic field, crystal axis, and polarization of the incident electric vector in a single experiment. The analysis is carried out by considering separately the polarization of the E vector perpendicular and parallel to the magnetic field. The attenuation coefficient β for the two cases is again obtained via Eq. (1) from the effective dielectric constant $\epsilon_{\text{eff}}=\epsilon'+i\epsilon''$. For the perpendicular polarization ϵ_{eff} is given by[1]

$$\epsilon_{(\text{eff})\perp}=\epsilon_{st}'-\frac{i}{\omega}\left(\sigma_{11}+\frac{\sigma_{12}^2}{\sigma_{22}+i\omega\epsilon_{st}'}\right)=\epsilon_{st}'-\frac{i}{\omega}\sigma_\perp, \quad (19)$$

and for the parallel polarization by

$$\epsilon_{(\text{eff})\parallel}=\epsilon_{st}'-\frac{i}{\omega}\sigma_{33}, \quad (20)$$

where the propagation is always along direction 2, magnetic field along direction 3, and the σ_{ij} are, of course, complex. The amplitude ratio for either polarization is then

$$\ln\left(\frac{E(B)}{E(0)}\right)_{\perp,\parallel}=[\beta(B)_{\perp,\parallel}-\beta_0]z. \quad (21)$$

For transverse polarization in the region of low losses, Eq. (21) becomes

$$\ln\frac{E(B)}{E(0)}=\tfrac{1}{2}z\left(\frac{\mu_0}{\epsilon_{st}'}\right)^{1/2}\text{Re}[\sigma_{11}(0)-\sigma_\perp]$$

$$=\tfrac{1}{2}z\left(\frac{\mu_0}{\epsilon_{st}'}\right)^{1/2}\frac{ne^2}{m^*}\frac{\omega_c^2\tau^3(1+\omega_c^2\tau^2-3\omega^2\tau^2+2\omega_p^2\tau^2)}{(1+\omega^2\tau^2)[(1+\omega_c^2\tau^2-\omega^2\tau^2+\omega_p^2\tau^2)^2+\omega^2\tau^2(2-\omega_p^2/\omega^2)^2]}, \quad (22)$$

where $\omega_p\equiv(ne^2/m^*\epsilon_{st}')^{1/2}$ is the classical plasma frequency. In order to retain the plasma terms, which are prominent in this configuration even in the low-loss region, the constant τ model is used, since the energy-dependent treatment yields a rather cumbersome and unrevealing expression. It is interesting to note that Eq. (22) displays two extrema when frequency rather than magnetic field is varied. When the plasma frequency is very small, Eq. (21) for the perpendicular polarization reduces to Eq. (6).

In the region of high losses corresponding to that defined in Sec. 3 the amplitude ratio becomes, for samples thicker than the skin depth,

$$\ln\frac{E(B)}{E(0)}=-\tfrac{1}{2}z\left(\frac{\mu_0\omega\sigma_0}{2}\right)^{1/2}\mu_H^2B^2\left(1-\frac{\langle\tau^3\rangle\langle\tau\rangle}{\langle\tau^2\rangle^2}-\frac{\omega\epsilon_{st}'}{\sigma_0}\right). \quad (23)$$

This differs from the expression for the Faraday configuration by the presence of the first and third terms in the bracket. The difference is analogous to that between dc magnetoresistance associated with the shorted and the open-circuit Hall fields, the latter case corresponding, of course, to the Voigt configuration. It should be pointed out that it is necessary to use the energy-dependent τ derivation, since in the constant τ approximation the major term of Eq. (23) disappears entirely.

The amplitude variation for the E vector parallel to the magnetic field gives a measure of longitudinal magnetoconductivity. In this case the expressions describing low- and high-loss situation will be given, respectively, by Eq. (6) and (12), with $\Delta\sigma'$ defined as $\sigma_{11}'(0)-\sigma_{33}'(B)$. Except in isotropic cases $\sigma_{33}(B)$ is, of course, generally not equal to $\sigma_{11}(0)$.

EXPERIMENTAL RESULTS AND DISCUSSION

A. The Faraday Configuration

We have studied experimentally the behavior of the amplitude ratio in the case of longitudinal propagation at 35 Gc/sec at room temperature, i.e., in the region $\tau^{-1}\gg\omega, \omega_c$, in silicon and germanium. All samples satisfy the condition under which Eq. (6) is valid, namely, $\epsilon''/\epsilon'\approx\omega_p^2/(\omega\tau^{-1})\ll1$. The apparatus designed for measuring the Faraday rotation[5] was adapted to study the effect. The instrument consists essentially of a cylindrical waveguide propagating the TE_{11} mode, which passes through an axial hole in the magnet pole-pieces and is terminated with an analyzer head capable of rotating about the direction of propagation. The sample, in the form of a disk, is placed at a waveguide discontinuity in the center of the field. Since the polarization ellipse rotates as a function of the magnetic field, the analyzer can be rotated to the position of maximum signal at each value of the field to obtain the amplitude. Every measurement is repeated for the reverse field direction, and the average taken, to cancel the error arising from possible zero-field ellipticity.

Faraday rotation can be measured simultaneously. A mode correction must be applied to obtain the corresponding plane wave rotation θ appearing in our equations.[8] For the TE_{11} mode propagating with small losses and far from cutoff this amounts to multiplying the observed guided rotation by the factor 1.18.

[8] H. Suhl and L. R. Walker, Phys. Rev. 86, 122 (1952).

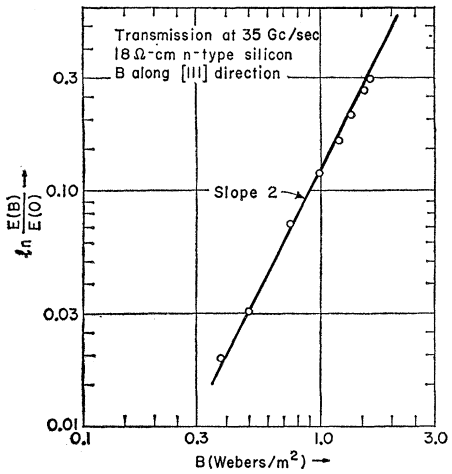

FIG. 1. The circles represent room temperature measurements of the amplitude ratio versus magnetic field for a typical n-type silicon sample, 5 mm thick. The straight line of slope 2 is drawn to illustrate the quadratic nature of the effect at lower fields. Note the small but systematic departure of experimental points from the B^2 dependence in the upper limit of the plot due to fourth order B terms, which gradually become important as μB is increased. The highest point corresponds to $\mu B \approx 0.2$.

1. *n-Type Silicon*

Typical data for n-type silicon as a function of magnetic field are shown in Fig. 1. As discussed in Sec. 5 above, the amplitude ratio in this material depends directly on the relative orientation of the field and the crystal. At this point it is convenient to define the quantity

$$\mu_{hkl} \equiv \left[\ln\frac{E(B)}{E(0)}\right]\left[\theta B\frac{\langle\tau^3\rangle}{\langle\tau^2\rangle\langle\tau\rangle}\right]^{-1}, \tag{24}$$

where hkl refer to the direction of the magnetic field relative to the crystal axes.

Using the results of Sec. 5 and the expression for θ in terms of m_1 and m_2,[9] we have, for n-type silicon,

$$\mu_{111} = \frac{e\langle\tau\rangle}{3}\left(\frac{1}{m_1}+\frac{2}{m_2}\right) = \frac{e\langle\tau\rangle}{m^*} \equiv \mu_d, \tag{25a}$$

and

$$\mu_{100} = \frac{3(m_1^2+m_1m_2+m_2^2)}{(m_1+2m_2)(2m_1+m_2)}\mu_d. \tag{25b}$$

The experimental results are summarized in Table I. Isotropic lattice scattering, which yields $\langle\tau^3\rangle/(\langle\tau^2\rangle\langle\tau\rangle) = 1.50$, was assumed in calculating the tabulated values of μ. Electron drift mobility for lightly doped silicon is known to be about 0.135 m²/V-sec,[10] which gives satisfactory agreement with our results. The theoretical value of μ_{100}/μ_{111}, obtained by using $m_1/m_2 = 5.16$,[11] also compares favorably with our results.

TABLE I. Comparison of theoretical and experimental values for oriented n-type silicon crystals. Thickness of the specimens is 1 cm for samples 1–5, 0.5 cm for sample 6.

Sample	ρ (Ω-cm)	hkl	μ_{hkl} (m²/V-sec)	μ_{100}/μ_{111} expt.	theor.
1	51	100	0.167	1.24	
2	46	111	0.135		
3	41	100	0.170	1.23	1.214
4	40	111	0.138		
5	24	100	0.153	1.21	
6	18	111	0.126		

[9] In the range considered here,
$\theta = \frac{1}{2}z(\mu_0/\epsilon_{si}')^{1/2}\sigma_0\mu_H B = \frac{1}{2}z(\mu_0/\epsilon_{si}')^{1/2}ne^3B\langle\tau^2\rangle\cdot(m_1+2m_2)/(3m_1m_2^2)$.

2. *Magnetodichroism*

As pointed out in Sec. 5, for B applied along crystal directions other than [100] and [111] in n-type silicon, $\sigma_{11} \neq \sigma_{22}$ and the above equations do not hold. In addition to its dependence on the direction of the magnetic field, the transmitted amplitude will now also depend on the orientation of the incident electric vector relative to the crystal axes, thus exhibiting a form of dichroism induced by the magnetic field.

TABLE II. Comparison of experimental results and theoretical estimates for n-type silicon crystal with B along the [110], and $E(0)$ along the [001] and [$\bar{1}$10] directions. Sample resistivity is 38 Ω-cm, thickness 1 cm. Theoretical values are obtained with Eq. (26).

Polarization qpr	μ_{110}^{qpr} (m²/V-sec)	$\mu_{110}^{qpr}/\mu_{100}$ expt.	theor.	$\mu_{110}^{\bar{1}10}/\mu_{110}^{001}$ expt.	theor.
001	0.165	1.01	1.00	0.75	0.74
$\bar{1}$10	0.123	0.75	0.74		

We measured the amplitude ratio at low fields in n-type silicon, with B along the [110] axis. Faraday rotation, which does not depend on the directions of B and E in the low-field limit, was also measured. We define μ_{hkl}^{qpr} in analogy with Eq. (24), with the subscript denoting, as before, the orientation of the magnetic field, and the superscript referring to the direction of polarization of the incident electric field. The results are given in Table II.

The theoretical values in Table II are estimated in the following manner. We calculate the conductivity tensor for n-type silicon in the coordinate system where axes x, y, and z correspond to direction [001], [$\bar{1}$10],

[10] E. M. Conwell, Proc. I.R.E. **46**, 1281 (1958).
[11] G. Dresselhaus, A. I. Kip, and C. Kittel, Phys. Rev. **98**, 368 (1955).

and [110], respectively. We then assume that, to calculate $\ln[E(B)/E(0)]_{110}{}^{001}$ and $\ln[E(B)/E(0)]_{110}{}^{\bar{1}10}$ we may use Eq. (6) with $[\sigma_{11}'(0)-\sigma_{xx}'(B)]$ and $[\sigma_{11}'(0)-\sigma_{yy}'(B)]$, respectively, substituted for $\Delta\sigma'$. The argument appears especially plausible for small rotations. The relation thus obtained is

$$\frac{\mu_{110}{}^{\bar{1}10}}{\mu_{110}{}^{001}}=\frac{m_1{}^2+4m_1m_2+m_2{}^2}{2(m_1{}^2+m_1m_2+m_2{}^2)}=\frac{\mu_{110}{}^{\bar{1}10}}{\mu_{100}}. \quad (26)$$

The agreement between the theoretical values obtained in this manner and the measurement is rather interesting. It should be pointed out that, unlike the more symmetric situations considered in this paper, in this orientation of B the ratio m_1/m_2 can thus be measured simply by rotating the sample about its axis. It would be very desirable to analyze this case rigorously using the approach of Donovan and Webster.[6]

3. *p-Type Germanium and Silicon*

Figure 2 shows the results obtained on p-type germanium as a function of the field. Note the rather pronounced departure of the effect from quadratic B dependence at fields beyond about 3 kG. This departure is also present in the $\ln[E(B)/E(0)]/(\theta B)$ curve, because the relative contribution of the saturating light-hole term to the amplitude ratio is greater by a factor m_1/m_2 than the corresponding contribution to rotation.

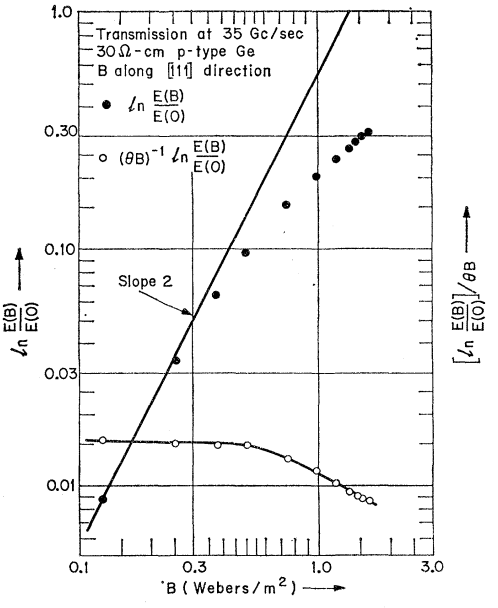

FIG. 2. Room-temperature measurements of the amplitude ratio versus magnetic field for a p-type germanium sample 3 mm thick are shown by solid circles. The straight line of slope 2 represents the low-field extrapolation and illustrates the pronounced departure of the data from the B^2 dependence beyond *ca.* 3 kG due to the saturation of the light-hole contribution. The highest point corresponds to $\mu_{d2}B\approx 2.3$. The open circles represent the amplitude ratios normalized by the simultaneously measured Faraday rotations. The flat portion of the solid curve, obtained from the low-field extrapolation of the data, is determined almost entirely by the light holes. This low-field value of the curve was used to estimate μ_{d2} in the text.

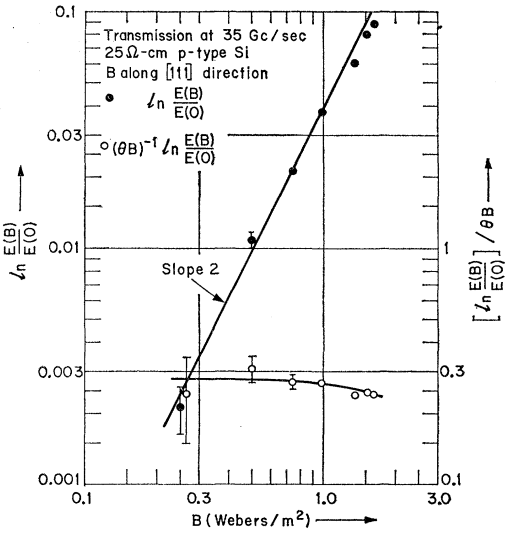

FIG. 3. Room-temperature measurements of the amplitude ratio versus magnetic field for a p-type silicon sample 5 mm thick are shown by solid circles. The straight line of slope 2 represents the low-field extrapolation. In contrast with p-type germanium, the effect barely begins to saturate in the upper limit of available magnetic fields due to the low mobilities involved. The highest experimental point corresponds to $\mu_{d2}B\approx 0.35$. The open circles represent the amplitude ratios normalized by the simultaneously measured Faraday rotations. The flat portion of the solid curve, obtained from the low-field extrapolation, was used to estimate the value of μ_{d2} in the text.

It can be shown that at low fields,

$$\left[\ln\frac{E(B)}{E(0)}\right]\left[\theta B\frac{\langle\tau^3\rangle}{\langle\tau^2\rangle\langle\tau\rangle}\right]^{-1}=\frac{e\langle\tau\rangle}{m_2}\left[1-\left(\frac{m_2}{m_1}\right)^{1/2}+\frac{m_2}{m_1}\right], \quad (27)$$

where the assumption $n_2/n_1\approx(m_2/m_1)^{3/2}$ is made. Applying Eq. (27) to our measurement, we obtain, for lattice scattering and $m_1/m_2=8$,[11] the light-hole-drift mobility $\mu_{d2}\equiv(e\langle\tau\rangle/m_2)=1.33$ m²/V-sec. Assuming that $\mu_{d2}=\mu_{d1}(m_1/m_2)$, and using the value of the heavy-hole mobility known from dc measurements, $\mu_{d1}=0.190$ m²/V-sec,[10] we obtain $\mu_{d2}=1.52$ m²/V-sec, in fair agreement with our measurement.

Experimental results obtained on p-type silicon are shown in Fig. 3. The amplitude ratio, and its rate of dropping off as a function of the field, are considerably smaller than the corresponding effects in germanium, due to the relatively small value of m_1/m_2 in silicon. The value of μ_{d2} obtained from the low-field results via Eq. (27) is 0.25 m²/V-sec. The value of μ_{d2} estimated from published data ($\mu_{d1}=0.048$ m²/V-sec,[10] $m_1/m_2=3.06$ [11]) is 0.15 m²/V-sec. The discrepancy shows the necessity of a more detailed treatment of p-type silicon than that presented here. It is seen on inspection that the limitations imposed by the assumption $\tau_1=\tau_2$, $n_1/n_2=(m_1/m_2)^{3/2}$ are considerably more serious when

m_1/m_2 is not very large. The warping of the heavy-hole band, not considered in this paper, will then also affect the result, because of the relative importance of the heavy-hole term in Eq. (27). Furthermore, it can be shown that the assumption $\tau_1=\tau_2$, used both in the interpretation of the present results and in deriving μ_{d2} from published data, is itself valid to a lesser degree in silicon than in germanium.[12] Finally, at room temperature the contribution from the split-off V_3 band is also considerably greater than in the case of germanium, and should be considered.

B. The Voigt Configuration

In order to compare the theory for this configuration with experiment, we will apply the results of Sec. B to the published far infrared experiments of Palik *et al.* on GaAs.[13] Their experiment was carried out in the Voigt configuration, with the electric vector orthogonal to the magnetic field. The situation is described by Eq. (22), which predicts the main features of the behavior observed by these authors.

Referring to Fig. 1 of Ref. 13, we note that the following properties of Eq. (22) are illustrated: (1) $E(B)>E(0)$ in the high-field limit. It should be emphasized that this follows directly from Eq. (22), and is not a result of an interference effect, as has been previously supposed.[13] (2) $E(B)<E(0)$ in the low-field limit, under the condition $\omega>\tau^{-1}$, $\omega>\omega_p$. (3) $E(B)=E(0)$ when $\omega_c^2\approx 3\omega^2-2\omega_p^2$. The effect of the plasma term is clearly illustrated in the quoted figure, where $\omega_p(A)>\omega_p(B)>\omega_p(C)$, A, B, and C referring to the three samples studied. This property, which may be exploited to estimate ω_p, should be useful in eliminating the error from the corresponding shift in the cyclotron resonance condition $\omega_c^2=\omega^2-\omega_p^2$.

SUMMARY AND CONCLUSION

The theoretical analysis of the magnetic-field dependence of free-carrier absorption has shown that this effect can provide useful information about transport properties of semiconductors, in particular about the scattering mechanism, effective mass anisotropy, and degenerate band parameters. The simplicity of equations involved indicates that, even in the region where the dependence on transport parameters is essentially similar to that of dc magnetoresistance, magnetoabsorption measurements can yield this information more directly. This property should be especially useful in studying complicated systems, e.g., degenerate bands. A practical feature of considerable importance is that these measurement can be performed without the use of electric contacts.

The experiments have demonstrated that the effect is sufficiently large to be easily measured even by relatively unsophisticated methods, and that the results are in agreement with the values of transport parameters published by other workers. A simple bridge technique can be expected to increase the precision substantially.

We have discussed in some detail the relation between transmission changes and the associated rotation of the plane of polarization occurring in the Faraday configuration, because this simplified the interpretation of our experimental data. The disadvantage of this relation is that, in the case of rotation of guided waves, it is necessary to apply a mode correction before using the plane wave-expressions. It may be more advantageous to correlate the effect with the total zero-field absorption instead. This correlation is shown by the equations for the amplitude ratio where β_0 appears explicitly. The essential aim of either procedure is to eliminate several unknowns from the measurement, e.g., the dielectric constant and the optical thickness. Application of the high-frequency methods to materials in powder form may thus be possible.

It should finally be briefly mentioned that the imaginary counterpart of magnetoabsorption, i.e., the magnetic-field dependence of the total phase shift, manifests similar behavior and can be analyzed in complete analogy with the present development, using $\alpha=\omega(\frac{1}{2}\mu_0)^{1/2}[(\epsilon'^2+\epsilon''^2)^{1/2}+\epsilon']^{1/2}$ in place of β. It can be easily shown that the effect, which essentially involves quadratic B terms of ϵ_{eff}', may be quite large when $\omega\tau$ is not negligible, and will exhibit a particularly strong dependence on the scattering mechanism through the high powers of τ appearing inside the average. Measurement of the total phase shift as a function of the field, in conjunction with the absorption measurement, would thus be of considerable interest.

ACKNOWLEDGMENTS

The authors express their thanks to Texas Instruments, Inc., for providing semiconductor materials used in the microwave measurements.

[12] See, for example, Harvey Brooks, *Advances in Electronics and Electron Physics* (Academic Press Inc., New York, 1955), Vol. 7, p. 152.

[13] E. D. Palik, J. R. Stevenson and R. F. Wallis, Phys. Rev. 124, 701 (1961).